VOL. 12, NO. 17, SEPTEMBER 2017 ISSN 1819-6608
ARPN Journal of Engineering and Applied Sciences

www.arpnjournals.com

EVALUATION OF POWER SYSTEM RESTORATION INDICES USING KRILL HERD ALGORITHM BASED OPTIMIZED PI+ CONTROLLER FOR A RESTRUCTURED POWER SYSTEM WITH FACTS DEVICES

K. Chandrasekar, B. Paramasivam and I. A. Chidambaram
Department of Electrical Engineering, Annamalai University, Annamalainagar, Tamil Nadu, India
E-Mail: chandrueeeap@gmail.com

ABSTRACT

This paper presents evaluation of Power System Restoration (PSR) Indices based on the Automatic Generation Control (AGC) assessment of two-area thermal reheat power system with FACTS devices in a restructured environment. These PSR indices indicate the ancillary service requirements to improve the efficiency of the physical operation of the power system with the increased transmission capacity in the network. In this study, a new control strategy the Proportional and Integral plus (PI^+) controllers are designed using Krill Herd (KH) algorithm for solving AGC problem in power system. The PI^+ controller uses a low-pass filter on the command signal to remove the transient's response over shoot. In this way, the integral gain can be raised to higher values and PI^+ controller is useful in applications for AGC loop. The recent advances in power electronics have led to the development of the FACTS devices such as Thyristor Controlled Phase Shifter (TCPS) and Static Synchronous Series Compensator (SSSC) are capable of controlling the network condition in a very fast and economical manner. The proposed PI^+ controllers are designed and implemented in two-area unequal interconnected reheat thermal power plants with FACTS devices are considered for simulation study and their optimum settings are obtained using KH algorithm employing Integral Square Error based fitness function. From the simulations results, the incorporation of FACTS devices can enhance the total transfer capability and decrease the line congestion and to ensure improved PSR Indices in order to provide good margin of stability.

Keywords: AGC, TCPS, SSSC, PI^+ controller, krill herd algorithm, power system restoration indices.

1. INTRODUCTION

Automatic Generation Control (AGC) is important in electric power system design and operation. The objective of the AGC in an interconnected power system is to maintain the frequency of each area within limits and to keep tie-line power flows within some pre-specified tolerances by adjusting the MW outputs of the generators so as to accommodate fluctuating load demands [1, 2]. The traditional AGC two-area interconnected power system is modified to take into account the effect of bilateral contracts on the dynamics [3-5]. Based on the bilateral transactions, a distribution company (Disco) has the freedom to contract with any available generation company (Genco) in its own or another control area. Currently, these transactions are done under the supervision of the Independent System Operator (ISO), Independent Contract Administrator (ICA) or other responsible organizations. There can be various combinations of contracts between each Disco and available Gencos on the other hand, each Genco can contract with various Discos. With the formation of Disco Participation Matrix (DPM) the visualization of contracts can be made easier. DPM is a matrix with the number of rows equal to the number of Gencos and the number of columns equal to the number of Discos in the system. Each entry in this matrix can be thought of as a fraction of a total load contracted by a Disco (Column) toward a Genco (row) [6].

A control strategy is needed to maintain constancy of frequency and tie-line power and also to achieve zero steady state error. Several classical controllers such as Integral (I), Proportional-Integral (PI), Integral-Derivative (ID), and Proportional-Integral-Derivative (PID) have been adopted in AGC and are practically works for better dynamic responses [7]. Unlike a pure Proportional controller, a Proportional plus Integral (PI) controller can track the step change and eventually reduce the error to zero. The PI controller employed to solve AGC problem and these controller gives the good response, reduces the oscillation and steady state error. Even though PI controllers have wide usages in controlling the Load Frequency Control (LFC) problems the Integral gain in PI controller is limited relatively to small values because of its high the overshoot in the transient's response. So that a new control strategy such as the Proportional and Integral plus (PI^+) controller was proposed and adopted in this study [8]. The PI^+ controller uses a low-pass filter on the command signal to remove the transient's response over shoot. The controller parameters plays a vital role for its performance, thus it should be tuned properly with suitable optimization techniques. Many evolutionary heuristic algorithms have been proposed in the area of AGC for better performance analysis by the researchers over past two decades such as Differential Evolution (DE) [9], Particle Swarm Optimisation (PSO) [10], Genetic Algorithm (GA) [11], Craziness-based PSO (CRPSO) [12] and Bacterial Foraging Optimization (BFO) algorithm [13] etc. However, they suffer from local optimisation problem, required long simulation time, complex algorithm etc. From literature survey the enhancement of power system performance not only depends on the control structure but

also on the well-tuned controllers. Therefore, modern evolutionary methods such as Krill Herd (KH) algorithm is a novel swarm intelligent algorithm which is inspired the herding behavior of the krill swarms. In the algorithm, three main factors define the position of the krill individuals that are movement induced by the presence of other individuals, foraging activity, and random diffusion [14-17]. In this study the proposed PI^+ controller is designed using KH algorithm and implemented for the two-area interconnected thermal reheat restructured power system.

Various series FACTS controllers can be used in series with tie-line of interconnected power systems to regulate the power flow and damp the inter-area oscillations through proposing a complementary damping controller. As a result of fast dynamic responses, series FACTS controllers such as Thyristor Controlled Phase Shifter (TCPS) [18] and Static Synchronous Series Compensator (SSSC) [19, 20] have been adopted in interconnected power systems to mitigate the area frequency and tie-line power oscillations. Large-scale power system when faces severe disturbance requires quick recovery of the power system and can somewhat be able to avoid blackouts with the black start units which can be able to produce power for the auxiliaries of the thermal units without black start capabilities. Under this situation a conventional frequency control i.e., a governor may no longer be able to compensate for such load changes due to the slow response. Therefore, in an inter area mode, damping out the critical electromechanical oscillations is essential and has to be implemented properly in an interconnected system. Proper monitoring of the system frequency deviations and remedial actions to overcome frequency excursions are more likely to protect the system before it enters an emergency mode of operation [21, 22]. This paper proposes computation of Power System Restoration (PSR) Indices based on the Automatic Generation Control (AGC) assessment of interconnected restructured power system without and with FACTS devices. The PSR indices are calculated based on the settling time and peak over shoot concept of the dynamic output responses of the system and the control input deviations of each area for different types of possible transactions and the necessary remedial measures to be adopted are also suggested.

2. AGC IN RESTRUCTURED POWER SYSTEM

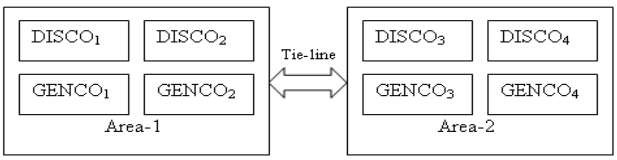

Fiureg-1. Schematic diagram of two-area system in restructured environment.

In the restructured competitive environment of power system, the Vertically Integrated Utility (VIU) no longer exists. The deregulated power system consists of generation companies (GENCOs), distribution companies (DISCOs), Transmissions companies (TRANSCOs) and Independent System Operator (ISO). GENCOs which will compete in a free market to sell the electricity they produce. The entities that will wheel this power between GENCOs and DISCOs have been designated as TRANSCOs. Although it is conceptually clean to have separate functionalities for the GENCOs, TRANSCOs and DISCOs, in reality there will exist companies with combined or partial responsibilities. Among these ancillary service controls one of the most important services to be enhanced is the Load-frequency control. The LFC in a deregulated electricity market should be designed to consider different types of possible transactions, such as poolco-based transactions, bilateral transactions and a combination of these two [6]. In the new scenario, a DISCO can contract individually with a GENCO for acquiring the power and these transactions will be made under the supervision of ISO. To make the visualization of contracts easier, the concept of "DISCO Participation Matrix" (DPM) is used which essentially provides the information about the participation of a DISCO in contract with a GENCO. In DPM, the number of rows has to be equal to the number of GENCOs and the number of columns has to be equal to the number of DISCOs in the system. Any entry of this matrix is a fraction of total load power contracted by a DISCO toward a GENCO. As a results total of entries of column belong to $DISCO_i$ of DPM is $\sum_i cpf_{ij} = 1$. Where *cpf* represents "Contract Participation Factor" and is like signals that carry information as to which the GENCO has to follow the load demanded by the DISCO. In this study two-area interconnected power system in which each area has two GENCOs and two DISCOs. Let $GENCO_1$, $GENCO_2$, $DISCO_1$, $DISCO_2$ be in area 1 and $GENCO_3$, $GENCO_4$, $DISCO_3$, $DISCO_4$ be in area 2 as shown in Figure-1. The corresponding DPM is given as follows [4-6].

$$DPM = \begin{bmatrix} D & I & S & C & O \\ cpf_{11} & cpf_{12} & cpf_{13} & cpf_{14} & G \\ cpf_{21} & cpf_{22} & cpf_{23} & cpf_{24} & E \\ cpf_{31} & cpf_{32} & cpf_{33} & cpf_{34} & N \\ cpf_{41} & cpf_{42} & cpf_{43} & cpf_{44} & C \\ & & & & O \end{bmatrix} \quad (1)$$

The actual and scheduled steady state power flow through the tie-line are given as

$$\Delta P_{tie1-2,\,scheduled} = \sum_{i=1}^{2}\sum_{j=3}^{4} cpf_{ij}\Delta P_{L\,j} - \sum_{i=3}^{4}\sum_{j=1}^{2} cpf_{ij}\Delta P_{L\,j} \quad (2)$$

$$\Delta P_{tie1-2,\,actual} = \left(2\pi T_{12}/s\right)\left(\Delta F_1 - \Delta F_2\right) \quad (3)$$

And at any given time, the tie-line power error $\Delta P_{tie1-2,\,error}$ is defined as

$$\Delta P_{tie1-2,\,error} = \Delta P_{tie1-2,\,actual} - \Delta P_{tie1-2,\,scheduled} \quad (4)$$

The error signal is used to generate the respective ACE signals as in the traditional scenario

$$ACE_1 = \beta_1 \Delta F_1 + \Delta P_{tie\,1-2,\,error} \quad (5)$$

$$ACE_2 = \beta_2 \Delta F_2 + \Delta P_{tie\,2-1,\,error} \quad (6)$$

3. APPLICATION OF FACTS DEVICES IN AGC

The stabilization of frequency oscillations in an interconnected power system becomes challenging when implemented in the future competitive environment. So advanced economic, high efficiency and improved control schemes are required to ensure the power system reliability. The conventional load-frequency controller may no longer be able to attenuate the large frequency oscillation due to the slow response of the governor. The recent advances in power electronics have led to the development of the Flexible Alternating Current Transmission Systems (FACTS). As these FACTS devices are capable of controlling the network condition in a very fast manner the usage of FACTS devices are more apt to improve the stability of power system. In this study, Thyristor Controlled Phase Shifter (TCPS) and Static Synchronous Series Compensator (SSSC) are considered and it has been found that they are capable of controlling the network conditions in a very fast and economical manner.

3.1 Mathematical modelling of TCPS devices

A TCPS is one of the FACTS devices that can change the relative phase angle between the system voltages therefore, the real power flow can be regulated to mitigate the frequency oscillations and enhance power system stability [18, 19]. The TCPS is found to be superior to the governor system in terms of high-speed performance. When a sudden load perturbation occurs in power system, the TCPS quickly start control to suppress the peak value of the transient frequency deviation, governor systems responsively compensated for the steady state error of frequency deviation.

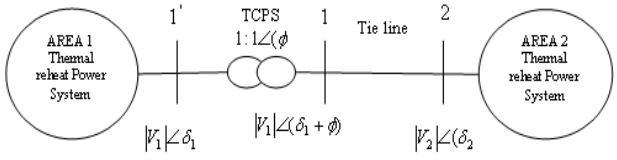

Figure-2. Incorporating TCPS device in a two area interconnected power system.

In this study the Figure-2 shows the schematic diagram of the two-area interconnected reheat thermal power system with TCPS in series with tie line. The mathematical model of a TCPS for stabilization of frequency oscillations is derived from the power flow control characteristics of the TCPS. Resistance of the tie-line is neglected. Without TCPS, the incremental tie-line power flow from area 1 to area 2 can be expressed [18].

$$\Delta P^{o}{}_{tie12}(s) = \frac{2\pi T^{o}{}_{12}}{s}\left[\Delta F_1(s) - \Delta F_2(s)\right] \quad (7)$$

When a TCPS is placed in series with the tie-line, as in Figure-2, the current flowing from area1 to area 2 can be written as

$$I_{12} = \left(\frac{|V_1|\angle(\delta_1 + \phi) - |V_2|\angle\delta_2}{jx_{12}}\right) \quad (8)$$

Where, x_{12} is the line reactance, V_1 and V_2 are the bus terminal voltages. The active and reactive power flows at bus 1 are

$$P_{tie12} + jQ_{tie12} = V_1 I^{*}$$
$$= |V_1|\angle(\delta_1 + \phi)\left(\frac{|V_1|\angle(\delta_1 + \phi) + |V_2|\angle\delta_2}{jx_{12}}\right) \quad (9)$$

Separating the real part of tie-line power in Equation (9)

$$P_{tie12} = \frac{|V_1||V_2|}{x_{12}}\sin(\delta_1 - \delta_2 + \phi) \quad (10)$$

In Equation (10) perturbing δ_1, δ_2 and ϕ from their nominal values δ^0, δ^0 and ϕ^0 respectively, we get

$$\Delta P_{tie12} = \frac{|V_1||V_2|}{x_{12}}\cos({\delta_1}^0 - {\delta_2}^0 + \phi^0)\sin(\Delta\delta_1 - \Delta\delta_2 + \Delta\phi) \quad (11)$$

But $(\Delta\delta_1 - \Delta\delta_2 + \Delta\phi)$ is very small and hence, $\sin(\Delta\delta_1 - \Delta\delta_2 + \Delta\phi) = (\Delta\delta_1 - \Delta\delta_2 + \Delta\phi)$,

Therefore,

$$\Delta P_{tie12} = \frac{|V_1||V_2|}{x_{12}}\cos({\delta_1}^0 - {\delta_2}^0 + \phi^0)(\Delta\delta_1 - \Delta\delta_2 + \Delta\phi) \quad (12)$$

$$\text{Let, } T_{12} = \frac{|V_1||V_2|}{x_{12}}\cos({\delta_1}^0 - {\delta_2}^0 + \phi^0) \quad (13)$$

Thus, Eq (12) reduces to

$$\therefore \Delta P_{tie12} = T_{12}(\Delta\delta_1 - \Delta\delta_2) + T_{12}\Delta\phi \quad (14)$$

It is known that

$$\Delta\delta_1 = 2\pi\int \Delta f_1 dt \quad and \quad \Delta\delta_2 = 2\pi\int \Delta f_2 dt \quad (15)$$

From the Equation (14) and Equation (15),

$$\Delta P_{tie12} = 2\pi T_{12}\left(\int \Delta f_1 dt - \int \Delta f_2 dt\right) + T_{12}\Delta\phi \quad (16)$$

Laplace Transform of Equation (16) is

$$\Delta P_{tie12}(s) = \frac{2\pi T_{12}}{s}\left[\Delta F_1(s) - \Delta F_2(s)\right] + T_{12}\Delta\phi(s) \quad (17)$$

It is evident from the Eq (17); tie line power flow can also be controlled by controlling the phase shifter angle$\Delta\phi$. The phase shifter angle $\Delta\phi$(s) can be represented as

$$\Delta\phi(s) = \frac{k\phi}{1+sT_{tcps}}\Delta Error_1(s) \quad (18)$$

Where kϕ is the Gain value of TCPS, T_{PS} is the time constant of TCPS unit. In this study, the input signal to the TCPS control logic is considered the frequency deviation of area 1 [ΔF_1]. Thus the tie-line power flow perturbation becomes

$$\Delta P_{tie12}(s) = \frac{2\pi T_{12}}{s}\left[\Delta F_1(s) - \Delta F_2(s)\right] + T_{12}\frac{k\phi}{1+sT_{tcps}}\Delta F_1(s) \quad (19)$$

3.2 Mathematical modelling of SSSC devices

Figure-3, Shows the two-area interconnected power system with a configuration of SSSC used for the proposed control design. It is assumed that a large load with rapid step load change has been experienced by area 1. This load change causes serious frequency oscillations in the system. Under this situation, the governors in an area 1 cannot sufficiently provide adequate frequency control. On the other hand, the area 2 has large control capability enough to spare for other area. Therefore, area 2 offers service for frequency stabilization in area 1 using the SSSC unit. Since SSSC is a series connected device, the power flow control effect is independent of the installed location. In the proposed design method, the SSSC unit uses the frequency deviation of area 1 as the local signal input. Therefore the SSSC unit is placed at the point near area 1. Moreover the SSSC unit is utilized as the energy transfer device from area 2 to area 1. As the frequency fluctuation in area 1 occurs, the SSSC unit will provide the dynamic control of the tie-line power by exploiting the system interconnections as the control channels and the frequency oscillation can be stabilized.

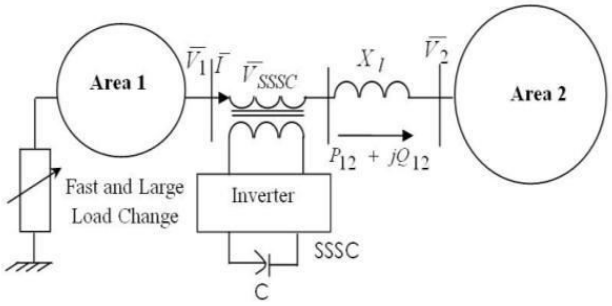

Figure-3. Incorporating SSSC device in a two area interconnected power system.

In this study, the mathematical model of the SSSC for stabilization of frequency oscillations is derived from the characteristics of power flow control of SSSC [19, 20]. By adjusting the output voltage of SSSC ($\bar{V}_{sssc}$), the tie-line power flow (P_{12}+jQ_{12}), can be directly controlled as shown in Figure-3. Since the SSSC fundamentally controls only the reactive power, then the phasor $\bar{V}_{sssc}$ is perpendicular to the phasor of line current $\bar{I}$, which can be expressed as

$$\bar{V}_{sssc} = jV_{sssc}\bar{I}/I \quad (20)$$

Where V_{sssc} and I are magnitudes of $\bar{V}_{sssc}$ and $\bar{I}$ respectively. Note that, Where $\bar{I}/I$ is a unit vector of line current. Therefore, the current $\bar{I}$ in Figure-3, can be expressed as

$$\bar{I} = (\bar{V}_1 - \bar{V}_2 - jV_{sssc}\bar{I}/I)/jX_l \quad (21)$$

Where X_l is the reactance of the tie line, $\bar{V}_1$ and $\bar{V}_2$ is the bus voltages at bus 1 and 2 respectively. The active power and reactive power flow through bus 1 are

$$P_{12} + jQ_{12} = \bar{V}_1\bar{I}^* \quad (22)$$

Where $\bar{I}^*$ is conjugate of $\bar{I}$, Substituting $\bar{I}$ from Equation (21) in Equation (22),

$$P_{12} + jQ_{12} = \frac{V_1V_2}{X_l}\sin(\delta_1 - \delta_2) - V_{sssc}\frac{\bar{V}_1\bar{I}^*}{X_lI} + j\left(\frac{V_1^2}{X_l} - \frac{V_1V_2}{X_l}\cos(\delta_1 - \delta_2)\right) \quad (23)$$

Where $\bar{V}_1 = V_1e^{j\delta_1}$ and $\bar{V}_2 = V_2e^{j\delta_2}$.

In Equation (23), the second term of right hand side $\bar{V}_1\bar{I}^*$ is $P_{12} + jQ_{12}$. As a result, the real part of Equation (23) gives

$$P_{12} = \frac{V_1V_2}{X_l}\sin(\delta_1 - \delta_2) - \frac{P_{12}}{X_lI}V_{sssc} \quad (24)$$

The second term of right hand side of Equation (24) is the active power controlled by SSSC. Here, it is assumed that V_1 and V_2 are constant, and the initial value of V_{SSSC} is zero. i.e. $V_{SSSC} = 0$ by linearzing Equation (23) about an initial operating point

$$\Delta P_{12} = \frac{V_1 V_2 \cos(\delta_{10} - \delta_{20})}{X_l}(\Delta\delta_1 - \Delta\delta_2) - \frac{P_{120}}{X_l I_o}\Delta V_{sssc} \quad (25)$$

Where subscript "0" denotes the value at the initial operating point, by varying the SSSC output voltage ΔV_{sssc}, the power output of SSSC can be controlled as. $\Delta P_{sssc} = -(P_{120} / X_l I_0)\Delta V_{sssc}$. Equation (25) implies that the SSSC is capable of controlling the active power independently. In this study, the SSSC is represented by the power flow controller where the control effect of active power by SSSC is expressed by ΔP_{sssc} instead of $-(P_{120} / X_l I_0)\Delta V_{sssc}$. Equation (25) can also be expressed as:

$$\Delta P_{12} = \Delta P_{T12} + \Delta P_{sssc} \quad (26)$$

$$\Delta P_{T12} = \frac{V_1 V_2 \cos(\delta_{10} - \delta_{20})}{X_l}(\Delta\delta_1 - \Delta\delta_2) = T_{12}(\Delta\delta_1 - \Delta\delta_2) \quad (27)$$

T_{12} is the synchronizing power co-efficient.

3.3 Structure of SSSC-based damping controller

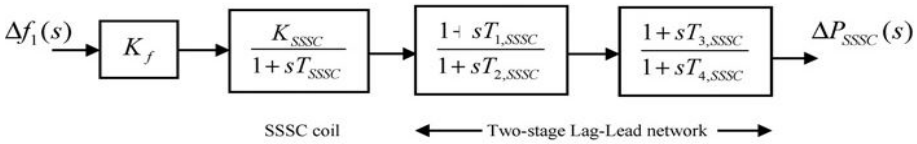

Figure-4. Structure of SSSC-based damping controller.

The active power controller of SSSC has a structure of the Lead-Lag compensator with output signal $\Delta P_{ref.}$ In this study the dynamic characteristics of SSSC is modeled as the first order controller with time constant T_{SSSC} It is to be noted that the injected power deviations of SSSC, ΔP_{sssc} acting positively in area 1 reacts negatively in area 2. Therefore ΔP_{sssc} flow into both area with different signs (+, -) simultaneously. The commonly used Lead-Lag structure is chosen in this study for the design of SSSC unit based supplementary damping controller as shown in Figure-4. The structures consist of a gain block, a washout block and two-stage phase compensation block. The phase compensation block provides the appropriate phase-lead characteristics to compensate for the phase lag between input and output signals. The input signals associated with oscillations is passed unchanged would modify the output. The input signal of the proposed SSSC-based controller is frequency deviations Δf and tie- line power deviations and the output is the change in control vector ΔP_{sssc}. From the view point of the washout function the value of washout time constant is not critical in Lead-Lag structured controllers and may be in the range of 1 to 20 seconds. Thus, there are control parameters of SSSC such as Ksssc, Tsssc, T_1, T_2, T_3 and T_4 to be optimized using KH algorithm.

4. DESIGN OF PROPORTIONAL-INTEGRAL PLUS (PI^+) CONTROLLERS

In PI controller K_P provides stability and high frequency response and K_I ensures that the average error is driven to zero. So no long term error, as the two gains are tuned. This normally provides high responsive systems. But the predominant weakness of PI controller is it often produces excessive overshoot to a step command. The PI controller lacks a windup function to control the integral value during saturation. But PI^+ control uses a low pass filter on the command signal to limit the overshoot. The Proportional and Integral plus (PI^+) controller as the name indicates is an enhancement to PI. Because of the overshoot, the integral gain in PI controllers is limited in magnitude. PI^+ control uses a low-pass filter on the command signal to remove overshoot. In this way, the integral gain can be raised to higher values. PI^+ controoler is useful in AGC applications.

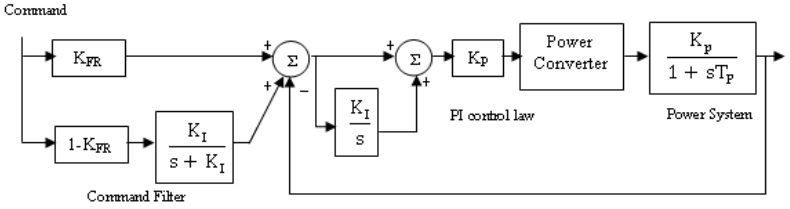

Figure-5. Block diagram for PI^+ control.

The PI+ controller is shown in Figure-5. The system has the PI controller with a command filter added. The degree to which a PI^+ controller filters the command signal is determined by the gain K_{FR}. When K_{FR} is 1, all filtering is removed and the controller is identical to a PI controller. Filtering is most severe when K_{FR} is zero. When K_{FR} is zero, command is filtered by $K_I/(s + K_I)$, which is a single-pole low-pass filter at the frequency K_I (in rad/sec). This case will allow the highest integral gain but also will most severely limit the controller command response. Typically, K_{FR} = 0 will allow an increase of almost three times in the integral gain but will reduce the bandwidth by about one-half when compared with K_{FR} = 1 (PI control). Finding the optimal value of K_{FR} depends on the application, but a value of 0.65 has been found to work in many applications. This value typically allows the integral gain to more than double while reducing the bandwidth by only 15%-20% [8]. K_I as the frequency of the command low-pass filter because it is excellent at canceling the peaking caused by the integral gain. PI^+ control is that it uses the command filter to attenuate the peaking caused by PI. The peaking caused by K_I can be canceled by the attenuation of a low-pass filter with a break of K_I. In Figure-5 the control law for PI^+ controller is represented as (28)

$$Control = K_P \left(command\left(K_{FR} + (1 - K_{FR}) \frac{K_I}{s + K_I} \right) - Feedback \right) \left(1 + \frac{K_I}{s} \right) \quad (28)$$

The gains parameters of controllers and frequency stabilisers are so selected such that some degree of relative stability, damping of electro-mechanical oscillations, minimum overshoots (OSs) and undershoots (USs) and lesser settling time are achieved. In the present work ACE of the respective areas are considered as input to the controllers and are defined in Equation (5) and (6), whereas the control inputs u_1 and u_2 are obtained with PI^+controller as Equation (29) and (30).

$$u_1 = K_{P1} \left(ACE_1 \left(K_{FR} + (1 - K_{FR}) \frac{K_{I1}}{s + K_{I1}} \right) - \Delta F_1 \right) \left(1 + \frac{K_{I1}}{s} \right) \quad (29)$$

$$u_2 = K_{P2} \left(ACE_2 \left(K_{FR} + (1 - K_{FR}) \frac{K_{I2}}{s + K_{I2}} \right) - \Delta F_1 \right) \left(1 + \frac{K_{I2}}{s} \right) \quad (30)$$

In the present work an Integral Square Error (ISE) criterion is used to minimize the objective function which is defined as in Equation (31).

$$J = \int_0^T \{ (\beta_1 \Delta f_1)^2 + (\beta_2 \Delta f_2)^2 + (\Delta P_{tie12})^2 \} \quad (31)$$

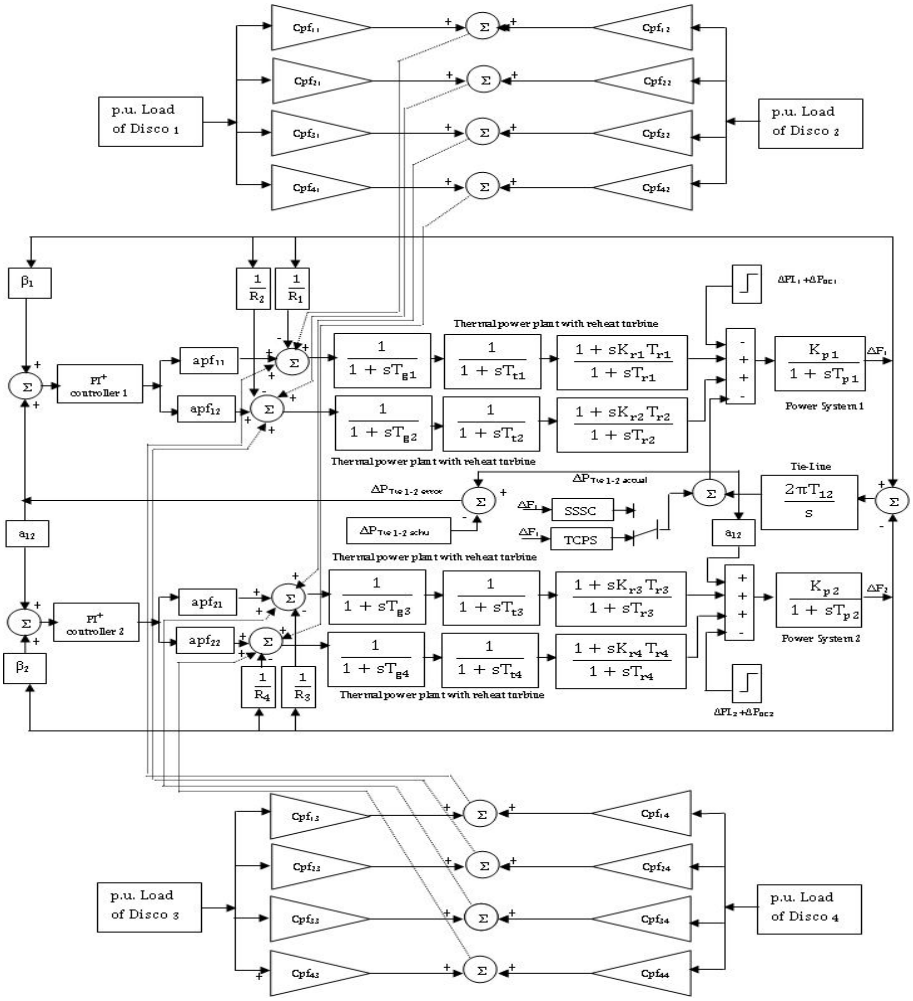

Figure-6. Linearized model of a two-area Thermal reheat interconnected power system in a restructured environment with FACTS devices.

The proportional Integral plus (PI^+) controller gain values (K_{p1}, K_{I1}, K_{p2}, K_{I2}) for a two-area thermal reheat interconnected power system in a restructured environment without and with FACTS devices are tuned using Krill Herd (KH) algorithm is shown in Figure-6. Where, K_p - Proportional gain, K_I - Integral gain, *ACE* - Area Control Error and u_1, u_2 - Control outputs of the respective areas. The relative simplicity of this controller is a successful approach towards the zero steady state error in the frequency of the system. With these optimized gain values the performance of the system is analyzed and various PSR indices are computed.

5. OVER VIEW OF KRILL HERD ALGORITHM

The Krill herd algorithm is a new optimization algorithm which is inspired the behavior of the krill swarms. Through an investigation of the herding behavior of krill swarms, the researchers find that the movement of krill swarms is to reach two main goals: (i) increasing krill density, and (ii) reaching food, so the herding behavior of increasing density and finding food is considered as a constrained optimization process [16, 17]. The location of a krill individual is affected by the following three factors: (i) Movement induced by other krill individuals; (ii) Foraging activity; and (iii) Random diffusion. So the location of the krill is expressed by the following Lagrangian model.

$$\frac{dx_i}{dt} = N_i + F_i + D_i \tag{32}$$

where N_i , F_i and D_i are the motion induced by other krill's, foraging activity and physical diffusion of the i^{th} krill individual respectively. The krill individuals always try to maintain a high density and move due to their mutual interaction with others. The movement of each krill individual is evaluated by the local, target and repulsive vector and may mathematically be expressed as follows:

$$N_i^{new} = N^{\max} \alpha_i + w_n \; N_i^{old} \tag{33}$$

where N^{max} is the maximum induced speed; α_i is the direction of motion which is approximately computed by the target effect, local effect and repulsive effect; w_n is the inertia weights of the motion induced and the range of [0, 1]; and N_i^{old} is the previous induced motion of the ith krill. Furthermore, α_i is defined as

$$\alpha_i = \alpha_i^{local} + \alpha_i^{target} \quad (34)$$

where α_i^{local} and α_i^{target} are the local effect provided by neighbours krill and target direction provided by the best krill individuals. The motion of a krill herd is influenced by two main effective factors: (i) the food location; and (ii) the previous experience about the food location. The expression of the motion can be stated as:

$$F_i = V_f \ \beta_i + \omega_f \ F_i^{old} \quad (35)$$

Where, V_f, ω_f and F_i^{old} are the forging speed, the inertia weight of the foraging motion, the last one, respectively. The physical diffusion of the krill individuals is a random process, and the motion associates with maximum diffusion speed and random directional vector. The equation of the physical diffusion can be defined by:

$$D_i = D_{\max} \ \delta \quad (36)$$

Where D_i *is* the maximum diffusion speed, δ is the random directional vector and its arrays are random values in [-1, 1]. The motion of krill swarm can be considered as a process toward the best fitness. So the position of a krill individual can be given by

$$x_i \ (t + \Delta t) = x_i(t) + \Delta t \ \frac{dx_i}{dt} \quad (37)$$

The parameter Δt is very important that can be treated as a scale factor of the speed vector. So it must be adjusted in terms of the optimization problem. The value of Δt is completely depends on the given search space.

5.1 Krill Herd algorithm for solving AGC application

The algorithmic steps of KHA applied to AGC problem are as follows:

Step 1: Initialization. Set the generaton counter t =1; initialize the population of krill randomly n_p, set the foraging speed V_f, the maximum diffusion speed D_{max}, the maximum induced speed N_{max} and the intertia weights w_n. Initialising PI^+control gain values (K_p, K_i) between minimum and maximum values.

Step 2: Evaluating fitness value of objective function (31) using current position of individual krill.

Step 3: Updating current krill's motion as follows: for i = 1: N_P, then do the following: Calculate motion of individual krill induced by other using (33). Calculate foraging motion using (35). Calculate physical diffusion using (36).

Step 4: Modify the position of individual krill's according to (37) and use current population for next step of generation.

Step 5: Increment the generation as t = t + 1. Checking whether controlled variables lie between minimum and maximum values or not. If present value is greater than maximum value, then keep maximum value as present solution; otherwise, go with present value. Similarly, if present value is less than minimum value, then keep minimum value as present solution and evaluating objective function using (31).

Step 6: Sorting current solution of control variables from best to worst and replace worst values by new modified set.

Step 7: Go to step 2 until termination criteria is fulfilled and sort the population from worst to best.

Step 8: End of optimisation loop. Finally, using the optimal setting of control variables, evaluate objective function using (31) and find transient specifications in terms of over/under shoot and settling time.

6. EVALUATION POWER SYSTEM RESTORATION INDICES

Power system restoration is well recognized as an important task to reduce the impact of a disturbance that occurs in power systems. The high level strategy of the System Restoration Plan is to restore the integrity of the interconnection as quickly as possible. The system restoration strategies are found closely related to the systems' characteristics. After analyzing the system conditions and characteristics of outages, system restoration planners or dispatchers will select the Power System Restoration (PSR) Indices which were obtained based on system dynamic performances and the remedial measures to be taken can be adjudged. In this study two-area thermal reheat interconnected power system in a restructured environment are considered when the system is operating in a normal condition with all Gencos units in operation and are one or more Gencos unit outage in any area. The various Power System Restoration indices (PSR_1, PSR_2, PSR_3, PSR_4, PSR_5, PSR_6, PSR_7 and PSR_8) are calculated as follows:

Step 1: The PSR_1 is obtained as the ratio between the settling time of frequency deviation in area 1 (ς_{s1}) and power system time constant (T_{p1}) of area 1

$$PSR_1 = \frac{\varsigma_{s1}}{T_{p1}} \quad (38)$$

Step 2: The PSR_2 is obtained as the ratio between the settling time of frequency deviation in area 2 (ς_{s2}) and power system time constant (T_{p2}) of area 2

$$PSR_2 = \frac{\varsigma_{s2}}{T_{p2}} \quad (39)$$

Step 3: The PSR_3 is obtained as the ratio between the settling time of Tie-line power deviation (ς_{s3}) and synchronous power coefficient T_{12}

$$PSR_3 = \frac{\varsigma_{s3}}{T_{12}} \quad (40)$$

Step 4: The PSR_4 is obtained as the peak value frequency deviation $\Delta F_1(\varsigma_p)$ response of area 1 exceeds the final value $\Delta F1\,(\varsigma_s)$

$$PSR_4 = \Delta F_1(\varsigma_p) - \Delta F_1(\varsigma_s) \quad (41)$$

Step 5: The PSR_5 is obtained as the peak value frequency deviation $\Delta F_2\ (\varsigma_p)$ response of area 2 exceeds the final value $\Delta F2\,(\varsigma_s)$

$$PSR_5 = \Delta F_2(\varsigma_p) - \Delta F_2(\varsigma_s) \quad (42)$$

Step 6: The PSR_6 is obtained as the peak value tie-line power deviation $\Delta P_{tie}\ (\varsigma_p)$ response exceeds the final value $\Delta P_{tie}\ (\varsigma_s)$

$$PSR_6 = \Delta P_{tie}(\varsigma_p) - \Delta P_{tie}(\varsigma_s) \quad (43)$$

Step 7: The PSR_7 is obtained from the peak value of the control input deviation $\Delta P_{c1}(\varsigma_p)$ response of area 1 with respect to the final value $\Delta P_{c1}(\varsigma_s)$

$$PSR_7 = \Delta P_{c1}(\varsigma_p) - \Delta P_{c1}\ (\varsigma_s) \quad (44)$$

Step 8: The PSR_8 is obtained from the peak value of the control input deviation $\Delta P_{c2}(\varsigma_p)$ response of area 2 with respect to the final value $\Delta P_{c2}(\varsigma_s)$

$$PSR_8 = \Delta P_{c2}(\varsigma_p) - \Delta P_{c2}\ (\varsigma_s) \quad (45)$$

7. SIMULATION RESULTS AND OBSERVATIONS

The proposed PI$^+$controllers are designed and implemented in two-area thermal reheat interconnected restructured power system for different type of transactions. In this test system consists of all the Gencos each area consists of thermal reheat unit with different capacity is shown in Figure-6. The nominal parameters are given in Appendix. The optimal solution of control inputs is taken an optimization problem, and the objective function in Eq (31) is derived using the frequency deviations of control areas and tie- line power changes. In bilateral based transactions, all Discos contracts with the Gencos for power as per the following DPM (1)

$$DPM = \begin{bmatrix} 0.5 & 0.25 & 0.5 & 0.4 \\ 0.2 & 0.25 & 0.2 & 0.2 \\ 0.0 & 0.3 & 0.2 & 0.25 \\ 0.3 & 0.2 & 0.1 & 0.15 \end{bmatrix} \quad (46)$$

In this case, the $Disco_1$, $Disco_2$, $Disco_3$ and $Disco_4$, demands 0.25pu.MW, 0.05 pu.MW, 0.25 pu.MW and 0.05 pu.MW from Gencos as defined by cpf in the DPM matrix. Each Gencos for thermal-thermal system participates in AGC as defined by the following area participation factor $apf_{11} = apf_{12} = 0.5$ and $apf_{21} = apf_{22} = 0.5$. Apart from the normal operating condition of the test systems few other case studies like outage Genco-4 in area 2 and uncontracted power demand in any area and Disco Participation Matrix (1) is considered. The PI$^+$ controller gains (K_{p1}, $K_{I1,}$ K_{p2}, K_{I2}) for each area tuned simultaneously with help of KH algorithm for the various case studies examples using both traditional and bilateral based AGC schemes with a wide range of load changes. The model of test systems under study are developed in MATLAB/Simulink environment and KHA is written in (.m) file. Owing to the random behaviour of KHA, it is impossible to judge effectiveness of same by a single run. About 50 trials have been made for selecting input parameters of same and following are found to be best for solving AGC problem: w_n= 0.7, w_f = 0.8, N = 75, V_f = 0.02, D^{max} = 0.005. The optimum PI$^+$ controller gain values for the test system are tuned for various case studies and are listed in the Table-1. To make the system be stable and to improve the dynamic behaviour of same, coordinated FACTS devices such as TCPS and SSSC are incorporated with PI$^+$controllers into the AGC loop. The corresponding optimum PI$^+$ controller gain values for different case studies as shown in Tables 2 and 3 respectively. Consider for a case-5, the optimized controller parameters of TCPS $k\phi$ =0.112, T_{tcps}=0.308. The optimal gain and time constant of SSSC based damping controller are found as K_{sssc} = 0.1; T_{sssc} = 0.035; $T_{1,\ sssc}$ = 0.425; $T_{2,\ sssc}$ = 0.411; $T_{3,\ sssc}$ = 0.783; $T_{4,\ sssc}$ = 0.125. The output dynamic responses of the two-area thermal reheat interconnected power system system have been shown in Figure-7. It is seen from Figure-7, it is evident that the dynamic responses have improved significantly with the use of FACTS device when connected in series with the tie-line. It can be observed that the oscillations in area frequencies and tie-line power deviations have decreased to a considerable extent as compared to that of the system without FACTS devices. Moreover SSSC devices could enhance the dynamic reeponces interms of frequency deviations of any area and tie-line powr oscillation as compared with TCPS devices. The various PSR indices are evaluated using Equation (38- 45) for the test system without FACTS and with TCPS and SSSC are tabulated in Tables 4, 5 and 6 respectively.

7.1. Power system restoration assessment

The main focus in this paper PSR indices are useful for system planners for restoration planning in advance.

(i) If $1.0 \leq PSR_1, PSR_2 \leq 5$ and $40 \leq PSR_3 \leq 50$, then the system subject to a large steady error for step load changes. Under a steady state condition, change in frequency of each area and change in tie-line power exchange will become more in some of case studies in Tables 4- 6. The integral control action are required based on the performance criteria such as ACE must be equal to zero at least one time in all 10-minute periods and average deviation of ACE from zero must be within specified limits based on a percentage of system generation for all 10-minutes periods. So that the above case studies, the integral controller gain (K_I) is made very large then only steady state frequency error reduces to zero. In other words, this means that speed regulation (R) should be made equal to zero, which is not desirable. Proportional control is not suitable for reducing the steady state error to zero. So that integral controller gain of each control area has to be increased causing the speed changer valve to open up widely. Thus the speed- changer position attains a constant value only when the frequency error is reduced to zero.

(ii) If $PSR_1, PSR_2 \geq 5$ and $PSR_3 \geq 50$ then the system required more amount of distributed generation requirement is needed and the FACTS devices are needed to improvement tie-line power oscillations. In this cases, the gain of the integrator is sufficiently high, over shoot will occur, increasing sharply as a function of the gain; this is highly undesirable. In the absence of integral control, one can sharply increase the gain of the closed- loop system and thereby improves the system response. However, the system will have a steady- state error. So that the Flexible Alternating Current Transmission (FACTS) devices coordinated with Energy Storage Systems (ESS) for LFC application has improve relatively stability of the power system and also to over come the draw back of the designing integral controller.

(iii) If $0.5 \leq PSR_4, PSR_5 \leq 1$ and $0.15 \leq PSR_7, PSR_8, \leq 0.2$ then the system required the stabilization of frequency oscillations in an interconnected power system. The conventional load-frequency controller may no longer be able to attenuate the large frequency oscillation due to the slow response of the governor for unpredictable load variations. Fast-acting energy storage systems having storage capacity in addition to the kinetic energy of the generator rotors is advisable to damp out the frequency oscillations. So that in deregulated system, regulation and load following are the two frequency-related ancillary services required for balancing the varying load with matching generation. Ancillary Services are defined as all those activities on the interconnected grid that are necessary to support the transmission of active power while maintaining reliable operation and ensuring the required degree of quality and security. These ancillary services are priced separately and ISO has to purchase these services from the ancillary service providers and distribute to the consumers. In a deregulated environment, any power system controls such as the LFC as an ancillary service acquires a principal role to maintain the electric system reliability at an adequate level and is becoming much more significant today in accordance with the complexity of interconnected power system.

(iv) If $0.05 \leq PSR_6 \leq 0.15$ then the FACTS devices are needed to improvement tie-line power oscillations. The recent advances in power electronics have led to the development of the Flexible Alternating Current Transmission Systems (FACTS). As these FACTS devices are capable of controlling the network condition in a very fast manner the usage of FACTS devices are more apt to improve the stability of power system. Several FACTS devices such as have been developed in recent decades. These FACTS devices are capable of controlling the network conditions in a very fast and economical manner.

(v) If $PSR_4, PSR_5 \geq 1$, $PSR_6 \geq 0.15$ and $PSR_7, PSR_8 \geq 0.2$ then the system is vulnerable and the system becomes unstable and may result to blackout. Small blackouts, involving only a few substations, can often be handled rather easily since they occur more often than the larger blackouts so the operators has more experience with them and the load can often be reconnected as soon as the operational reserves are able to meet the demand. Larger blackouts, affecting the whole or significant parts of the power system, are much harder to restore since large parts of the power system need to be energized and a significant part of the generating units will not be available. In order to handle restoration situations the operators have prepared restoration plans and guidelines for some typical blackout situations. The operators have to adopt these to the current situation. Two major strategies in power system restoration can be defined, bottom up vs. top down. Bottom up means that several smaller electrical islands are started in parallel; these are then used to energize the transmission system. The need to synchronize the islands can slow down the process. Top down means that the transmission system is energized from one point and all the lower voltage levels are energized from the transmission system and the whole energized power system is kept synchronized.

Table-1. Optimal PI^+ controller gain values using KH algorithm for two-area thermal reheat power system with corresponding load demand change.

Test system	PI^+controller gain values in Area 1 with K_{FR} = 0.65		PI^+ controller gain values in Area 2 with K_{FR} = 0.65		Load demand in pu.MW				uncontracted load demand in pu MW	
	K_{P1}	K_{I2}	K_{P2}	K_{I2}	$Disco_1$	$Disco_2$	$Disco_3$	$Disco_4$	Area 1	Area 2
Case 1	0.392	0.543	0.236	0.227	0.15	0.15	0.0	0.0	0.0	0.0
Case 2	0.411	0.447	0.304	0.234	0.15	0.15	0.0	0.0	0.05	0.0
Case 3	0.474	0.508	0.342	0.248	0.15	0.15	0.0	0.0	0.0	0.05
Case 4	0.493	0.452	0.354	0.251	0.15	0.15	0.0	0.0	0.05	0.05
Case 5	0.437	0.493	0.361	0.253	0.25	0.05	0.25	0.05	0.0	0.0
Case 6	0.403	0.575	0.219	0.311	0.25	0.05	0.25	0.05	0.1	0.0
Case 7	0.436	0.591	0.221	0.328	0.25	0.05	0.25	0.05	0.0	0.1
Case 8	0.441	0.597	0.337	0.267	0.25	0.05	0.25	0.05	0.1	0.1
Case 9	0.457	0.585	0.353	0.343	0.08	0.22	0.08	0.22	0.0	0.0
Case 10	0.464	0.667	0.283	0.364	0.08	0.22	0.08	0.22	0.15	0.0
Case 11	0.484	0.631	0.374	0.286	0.08	0.22	0.08	0.22	0.0	0.15
Case 12	0.501	0.688	0.366	0.323	0.08	0.22	0.08	0.22	0.15	0.15

Table-2. Optimal PI^+ controller gain values using KH algorithm for two-area thermal reheat power system with TCPS dervices for the corresponding load demand change.

Test system	PI^+controller gain values in Area 1 with K_{FR} =0.65		PI^+ controller gain values in Area 2 with K_{FR} =0.65		Load demand in pu.MW				uncontracted load demand in pu MW	
	K_{P1}	K_{I2}	K_{P2}	K_{I2}	$Disco_1$	$Disco_2$	$Disco_3$	$Disco_4$	Area 1	Area 2
Case 1	0.381	0.585	0.223	0.248	0.15	0.15	0.0	0.0	0.0	0.0
Case 2	0.394	0.467	0.292	0.256	0.15	0.15	0.0	0.0	0.05	0.0
Case 3	0.452	0.527	0.312	0.261	0.15	0.15	0.0	0.0	0.0	0.05
Case 4	0.498	0.474	0.343	0.272	0.15	0.15	0.0	0.0	0.05	0.05
Case 5	0.427	0.518	0.348	0.269	0.25	0.05	0.25	0.05	0.0	0.0
Case 6	0.382	0.588	0.211	0.323	0.25	0.05	0.25	0.05	0.1	0.0
Case 7	0.407	0.621	0.218	0.334	0.25	0.05	0.25	0.05	0.0	0.1
Case 8	0.423	0.646	0.326	0.276	0.25	0.05	0.25	0.05	0.1	0.1
Case 9	0.439	0.673	0.345	0.362	0.08	0.22	0.08	0.22	0.0	0.0
Case 10	0.451	0.699	0.278	0.381	0.08	0.22	0.08	0.22	0.15	0.0
Case 11	0.476	0.657	0.361	0.294	0.08	0.22	0.08	0.22	0.0	0.15
Case 12	0.485	0.693	0.358	0.346	0.08	0.22	0.08	0.22	0.15	0.15

Table-3. Optimal PI^+ controller gain values using KH algorithm for two-area thermal reheat power system with SSSC for the corresponding load demand change.

Test system	PI^+controller gain values in Area 1 with K_{FR} =0.65		PI^+ controller gain values in Area 2 with K_{FR} =0.65		Load demand in pu.MW				uncontracted load demand in pu MW	
	K_{P1}	K_{I2}	K_{P2}	K_{I2}	$Disco_1$	$Disco_2$	$Disco_3$	$Disco_4$	Area 1	Area 2
Case 1	0.361	0.592	0.218	0.275	0.15	0.15	0.0	0.0	0.0	0.0
Case 2	0.375	0.471	0.273	0.282	0.15	0.15	0.0	0.0	0.05	0.0
Case 3	0.436	0.529	0.308	0.284	0.15	0.15	0.0	0.0	0.0	0.05
Case 4	0.482	0.482	0.334	0.293	0.15	0.15	0.0	0.0	0.05	0.05
Case 5	0.416	0.541	0.341	0.276	0.25	0.05	0.25	0.05	0.0	0.0
Case 6	0.363	0.594	0.208	0.354	0.25	0.05	0.25	0.05	0.1	0.0
Case 7	0.401	0.633	0.211	0.361	0.25	0.05	0.25	0.05	0.0	0.1
Case 8	0.417	0.651	0.322	0.288	0.25	0.05	0.25	0.05	0.1	0.1
Case 9	0.428	0.678	0.327	0.373	0.08	0.22	0.08	0.22	0.0	0.0
Case 10	0.443	0.708	0.264	0.388	0.08	0.22	0.08	0.22	0.15	0.0
Case 11	0.458	0.669	0.345	0.314	0.08	0.22	0.08	0.22	0.0	0.15
Case 12	0.467	0.701	0.347	0.373	0.08	0.22	0.08	0.22	0.15	0.15

Table-4. Power System Restoration Indices for two-area thermal reheat power system using PI^+ controller with different types of case studies.

Test system	PSR indices based on settling time (ς_s)			FRI based on peak over/ under shoot (M_p)			FRI based on control input deviation (ΔP_c)	
	PSR_1	PSR_2	PSR_3	PSR_4	PSR_5	PSR_6	PSR_7	PSR_8
Case 1	0.841	0.821	38.09	0.334	0.292	0.031	0.125	0.095
Case 2	0.903	0.843	39.68	0.539	0.381	0.044	0.212	0.104
Case 3	0.875	0.918	42.87	0.411	0.436	0.049	0.125	0.229
Case 4	1.183	1.323	48.34	0.594	0.701	0.072	0.206	0.218
Case 5	0.897	0.858	36.13	0.306	0.398	0.056	0.112	0.051
Case 6	0.911	0.883	37.68	0.521	0.451	0.059	0.221	0.104
Case 7	0.913	0.955	40.17	0.364	0.611	0.066	0.123	0.118
Case 8	1.206	1.284	48.61	0.602	0.943	0.068	0.212	0.134
Case 9	1.372	1.442	52.88	0.501	0.512	0.129	0.181	0.156
Case 10	1.687	1.583	53.08	0.556	0.608	0.145	0.189	0.163
Case 11	1.503	1.727	56.34	0.569	0.833	0.148	0.182	0.167
Case 12	1.704	1.764	56.92	1.183	1.119	0.163	0.213	0.181

Table-5. Power system restoration Indices for two-area thermal reheat power system using PI^+ controller with TCPS for different types of case studies.

Test system	PSR indices based on settling time (ς_s)			FRI based on peak over/ under shoot (M_p)			FRI based on control input deviation (ΔP_c)	
	PSR_1	PSR_2	PSR_3	PSR_4	PSR_5	PSR_6	PSR_7	PSR_8
Case 1	0.806	0.801	27.09	0.323	0.279	0.024	0.117	0.086
Case 2	0.843	0.808	28.51	0.532	0.372	0.036	0.204	0.098
Case 3	0.801	0.861	31.18	0.403	0.419	0.041	0.119	0.222
Case 4	1.134	1.282	37.25	0.581	0.696	0.059	0.201	0.208
Case 5	0.821	0.822	25.18	0.253	0.342	0.048	0.092	0.046
Case 6	0.878	0.844	26.29	0.469	0.401	0.051	0.211	0.099
Case 7	0.871	0.916	29.45	0.302	0.567	0.056	0.111	0.108
Case 8	1.164	1.227	37.24	0.558	0.901	0.058	0.205	0.126
Case 9	1.183	1.359	48.72	0.407	0.409	0.106	0.159	0.141
Case 10	1.528	1.428	49.08	0.466	0.521	0.127	0.173	0.152
Case 11	1.201	1.619	51.47	0.514	0.719	0.134	0.166	0.156
Case 12	1.608	1.702	54.08	1.118	1.022	0.143	0.191	0.169

Table-6. Power system restoration Indices for two-area thermal reheat power system using PI^+ controller with SSSC for different types of case studies.

Test system	PSR indices based on settling time (ς_s)			FRI based on peak over/ under shoot (M_p)			FRI based on control input deviation (ΔP_c)	
	PSR_1	PSR_2	PSR_3	PSR_4	PSR_5	PSR_6	PSR_7	PSR_8
Case 1	0.804	0.798	26.03	0.322	0.278	0.023	0.116	0.085
Case 2	0.836	0.804	27.48	0.531	0.371	0.035	0.203	0.097
Case 3	0.798	0.855	30.12	0.402	0.418	0.038	0.118	0.221
Case 4	1.127	1.274	36.17	0.579	0.694	0.057	0.198	0.207
Case 5	0.818	0.816	24.09	0.251	0.338	0.047	0.091	0.045
Case 6	0.864	0.837	25.24	0.468	0.397	0.049	0.209	0.098
Case 7	0.859	0.914	28.32	0.301	0.565	0.055	0.108	0.107
Case 8	1.153	1.218	36.38	0.557	0.896	0.056	0.204	0.124
Case 9	1.172	1.343	47.61	0.406	0.407	0.104	0.158	0.138
Case 10	1.516	1.417	48.04	0.463	0.519	0.125	0.172	0.151
Case 11	1.198	1.608	50.37	0.512	0.718	0.133	0.165	0.155
Case 12	1.597	1.697	52.02	1.115	1.021	0.142	0.188	0.166

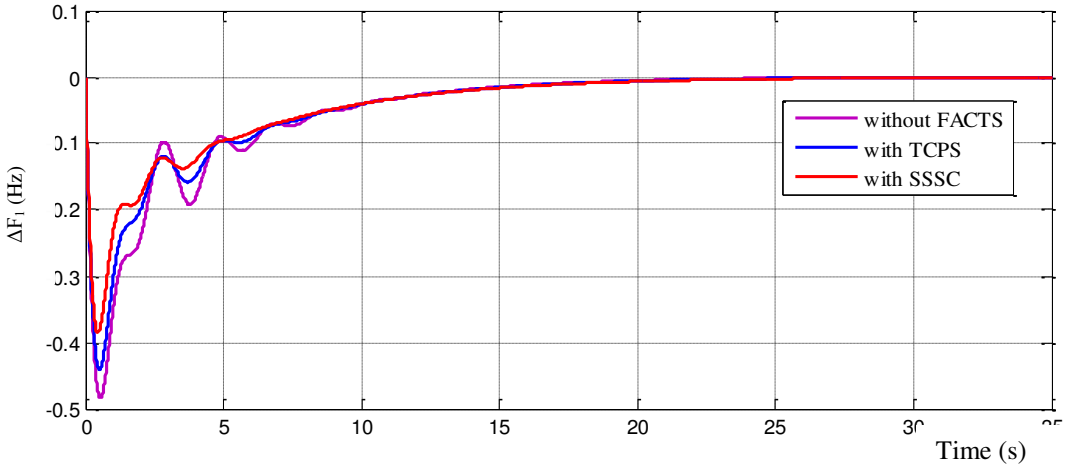

Figure-7(a). ΔF_1 (Hz) Vs Time(s).

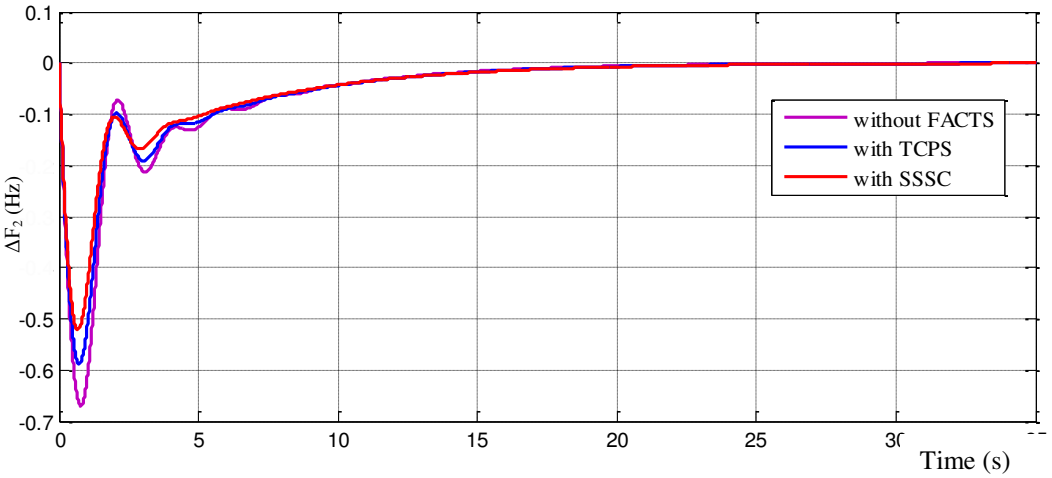

Figure-7(b). ΔF_2 (Hz) Vs Time (s).

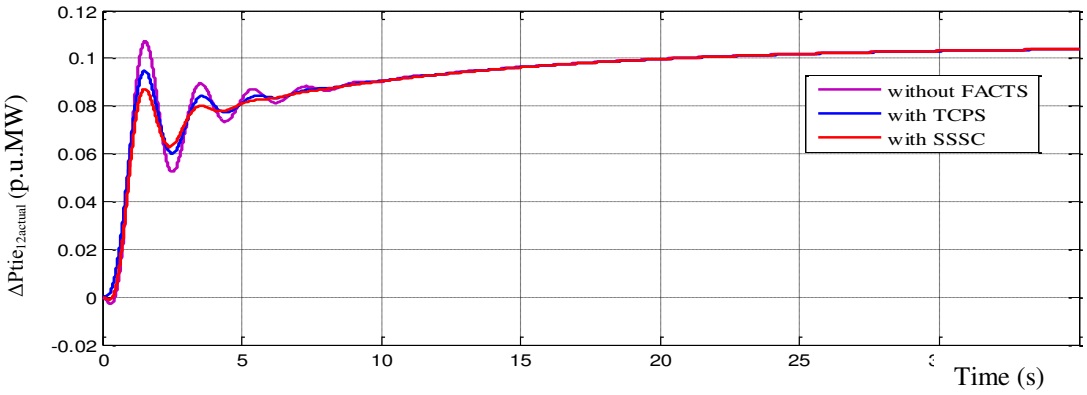

Figure-7(c). $\Delta Ptie_{12,\ actual}$ (p.u.MW) Vs Time (s).

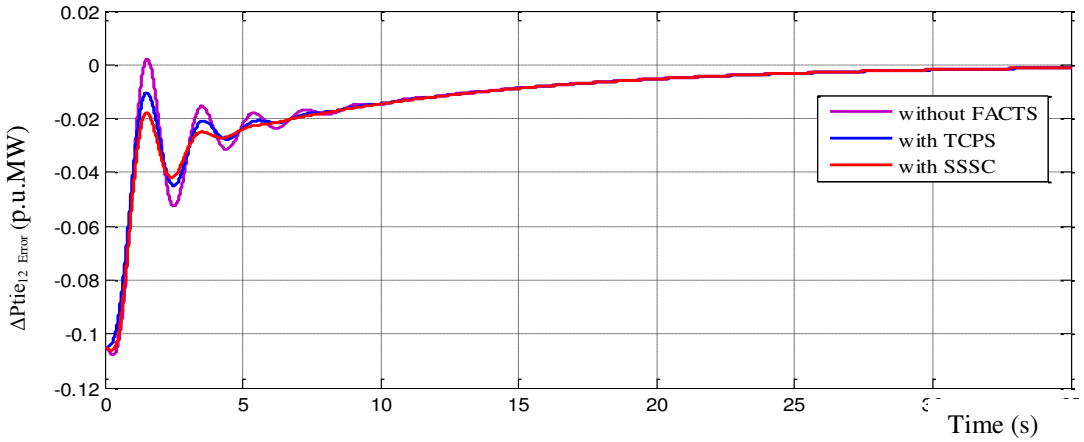

Figure-7(d). $\Delta Ptie_{12,\ Error}$ (p.u.MW) Vs Time (s).

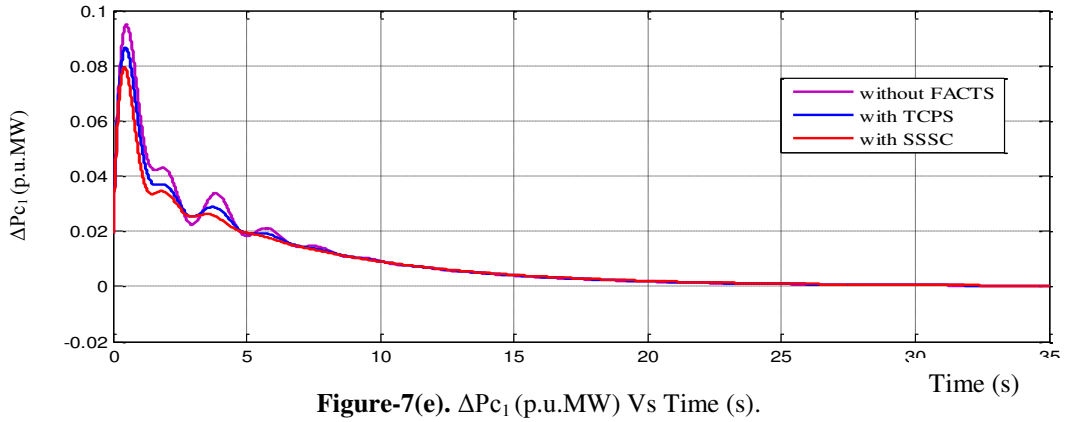

Figure-7(e). ΔPc_1 (p.u.MW) Vs Time (s).

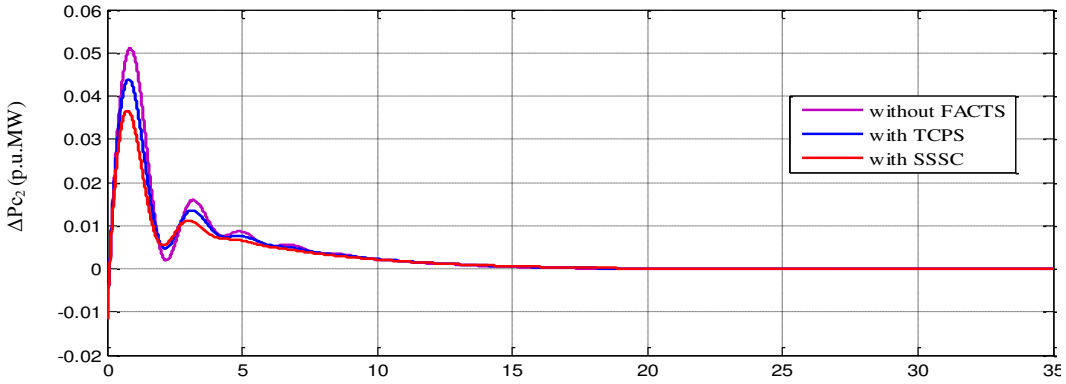

Figure-7(f) ΔPc_2 (p.u.MW) Vs Time (s).

Figure-7. Dynamic responses of the frequency deviations, tie- line power deviations, and Control input deviations for a two area thermal reheat power system without and with FACTS using PI^+ controllers (case-5).

8. CONCLUSIONS

A systematic method has been suggested to incorporate few FACTS devices such as TCPS and SSSC to improve the dynamic performance of a two area thermal reheat interconnected restructured power system. Analysis reveal that with the use of TCPS and SSSC devices, the oscillations are perfectly damped out and also the amplitudes of the deviations in frequency and tie-line power are reduced considerably when compared to those without FACTS devices. The PI^+ controllers are designed using KH algorithm and implemented in two area thermal reheat interconnected power system for different types of transactions. The PI^+ control uses a low-pass filter on the command signal to remove overshoot. In this way, the integral gain can be raised to higher values. PI^+ controller is useful in applications for AGC. The simulation results demonstrate that KH algorithm is able to reach the optimal solution irrespective of the large variation with a faster

convergence rate. From the simulated results it is observed that the PSR indices calculated for a test system with FACTS devices using PI^+ controller indicates that more sophisticated control for a better restoration of the power system output responses and to ensure improved PSR indices in order to provide good margin of stability.

ACKNOWLEDGEMENT

The authors wish to thank the authorities of Annamalai University, Annamalainagar, Tamilnadu, India for the facilities provided to prepare this paper.

REFERENCES

[1] Priyanka Sharma. 2014. AGC Strategies-A Review. International Journal of Engineering Research-Online. 2(4): 68-77.

[2] Naimul Hasan. 2012. An Overview of AGC Strategies in Power System. International Journal of Emerging Technology and Advanced Engineering. 2(8): 56-64.

[3] Shital M. Pujara and Chetan D. Kotwa. 2016. An Inclusive Review on Load Frequency Control in Deregulated Market. International Journal on Electrical Engineering and Informatics. 8(3): 595-611.

[4] Mukta and Balwinder Singh Surjan. 2013. Load Frequency Control of Interconnected Power System in Deregulated Environment: A Literature Review. International Journal of Engineering and Advanced Technology. 2(3): 435-441.

[5] Pardeep Nain, K.P. Singh Parmar and A.K. Singh. 2013. Automatic Generation Control of an Interconnected Power System before and After Deregulation. International Journal of Computer Applications. 61(15): 11-16.

[6] V. Donde, M. A. Pai, I. A. Hiskens. 2001. Simulation and optimization in an AGC system after deregulation. IEEE Transactions on Power Systems. 16(3): 481-489.

[7] Lalit Chandra Saikia, J. Nanda, S. Mishra. 2011. Performance comparison of several classical controllers in AGC for multi-area interconnected thermal system. International Journal of Electrical Power & Energy Systems. 33: 394-401.

[8] George Ellis. 2004. Control System Design guide, 3rd edition, Elsevier Academic Press, California.

[9] Routh U.K., Kumar R., Panda S. 2013. Design and analysis of differential evolution algorithm based automatic generation control for interconnected power system. Ain Shams Engineering Journal. 4(3): 409-421.

[10] H. Shayeghi, A. Pirayeshnegab, A. Jalili and H.A. Shayanfar. 2009. Application of PSO Technique for GEP in Restructured Power Systems. Energy Conversion and Management. 50: 2127- 2135.

[11] Gayadhar Panda, Sidhartha Panda and C. Ardil. 2010. Automatic Generation Control of Multi-Area Electric Energy Systems Using Modified GA. World Academy of Science, Engineering and Technology. 63: 717-725.

[12] H. Gozde and M. C. Taplamacioglu. 2011. Automatic Generation Control Application with Craziness based Particle Swarm Optimization in a Thermal Power System. Electrical Power and Energy Systems. 33: 8-16.

[13] B. Paramasivam and I.A. Chidambaram. 2010. Bacterial Foraging Optimization Based Load Frequency Control of Interconnected Power Systems with Static Synchronous Series Compensator. International Journal of Latest Trends in Computing. 1(2): 7-13.

[14] A .H. Gandomi and A. H Alavi. 2012. Krill herd: a new bio-inspired optimization algorithm. Communications in Nonlinear Science and Numerical Simulation. 17(12): 4831-4845.

[15] L. Guo, G. G. Wang, A. H. Gandomi, A.H. Alavi and H. A Duan. 2014. New improved krill herd algorithm for global numerical optimization. Neurocomputing. 138: 392-402.

[16] Songwei Huang, Lifang He, Xu Si, Yuanyuan Zhang and Pengyu Hao. 2016. An Effective Krill Herd Algorithm for Numerical Optimization. International Journal of Hybrid Information Technology. 9(7): 127-138.

[17] Dipayan Guha, Provas Kumar Roy and Subrata Banerjee. 2016. Krill herd algorithm for automatic generation control with flexible AC transmission system controller including superconducting magnetic energy storage units. The Journal of Engineering. pp. 1-15.

[18] Parmar KPS, Majhi S, Kothari DP. 2012. LFC of an interconnected power system with thyristor controlled phase shifter in the tie line. International Journal of Computer Application. 41(9): 27-32.

[19] Subbaramaiah K. 2011. Comparison of performance of SSSC and TCPS in automatic generation control of hydrothermal system under deregulated scenario. International Journal of Electrical and Computer Engineering (IJECE). 1(1): 21-30.

[20] Darabian M, Jalilvand A. 2013. SSSC and TCPS based hydrothermal system to improve dynamic performance via FABFM. International Journal of Automation Power Engineering (IJAPE). 2(5): 293-302.

[21] Yutian Liu, Rui Fan, Vladimir Terzija. 2016. Power system restoration: a literature review from 2006 to 2016. J. Mod. Power Syst. Clean Energy. 49(3): 332-341.

[22] R. Thirunavukarasu, I.A. Chidambaram. 2016. PI^2 controller based coordinated control with Redox Flow Battery and Unified Power Flow Controller for improved Restoration Indices in a deregulated power system. Ain Shams Engineering Journal. 7: 1011-1027.

[23] Jalili H., Shayeghi N.M., Tabatabaei. 2011. Fuzzy PID controller base on LFC in the deregulated power system including SMES. International Journal on Technical and Physical Problems of Engineering. 3(3): 38-47.

APPENDIX - A

A1. Control area parameter [23].

Parameters	**Area 1**	**Area 2**
k_p (Hz/p.u.MW)	120	72
T_p (sec)	20	14.3
β (p.u.MW / Hz)	0.8675	0.785
T_{ij} (p.u.MW / Hz)	$T_{12} = 0.545$	
F (Hz)	60	
a_{12}	-1	

A2. Gencos parameter (Thermal generating unit) [23].

MVA$_{Base}$ (1000 MW) **Parameters**	**Gencos** (k in area i)			
	1-1	1-2	2-1	2-2
Rate (MW)	1000	1100	800	900
T_g (sec)	0.06	0.06	0.07	0.08
T_t (sec)	0.36	0.44	0.42	0.4
T_r (sec)	10	10	10	10
K_r	0.5	0.5	0.5	0.5
R (Hz / p.u.MW)	2.4	2.5	3.3	2.4
apf	0.5	0.5	0.5	0.5

A3. Data for FACTS devices [19, 20].

Devices	**Parameters value**
TCPS	T_{ps} = 0.5 s, Kφ = 1.5 rad / Hz, Φmax = 10º, Φmin = - 10º
SSSC	T_{SSSC} = 0.05 s; T_w = 10 s